A Luenberger State Observer for Simultaneous Estimation of Speed and Rotor Resistance in sensorless Indirect Stator Flux Orientation Control of Induction Motor Drive

Mabrouk Jouili[1], Kamel Jarray[2], Yassine Koubaa[1] and Mohamed Boussak[3], Senior Member, IEEE

[1] Research Unit of Automatic Control (UCA), University of Sfax, National Engineering School of Sfax (ENIS), Sfax, B.P. 1173, 3038 Sfax, Tunisia

[2] Research Unit of Modeling, Analysis and Control of Systems (MACS), University of Gabès, National Engineering School of Gabès (ENIG), Gabès 6029, Tunisia

[3] Laboratoire des Sciences de l'Information et des Systèmes (LSIS), University of Aix Marseille III, Ecole Centrale de Marseille (ECM), Marseille, UMR 6168, France

Abstract

The primary objective of this paper is to implement a sensorless indirect stator field oriented control (ISFOC) of induction motor drive with rotor resistance tuning. Indeed, the proposed method for simultaneous rotor speed and rotor resistance estimation is based on Luenberger observer (LO). In order to estimate the rotor speed and the rotor resistance, an adaptive algorithm based on Lyapunov stability theory by using measured and estimated stator currents and estimated stator flux is proposed. The suggested control scheme, as a result, achieves a sound performance with computational complexity reduction obtained by using the analytical relation to determine the LO gain matrix. Again, the observer is simple and robust, when compared with the previously developed observers, and suitable for online implementation. For current regulation, however, this paper suggests a conventional Proportional-Integral (PI) controller with feed-forward compensation terms in the synchronous frame. Owing to its advantages, an Integral-Proportional (IP) controller is used for rotor speed regulation. The design, analysis, and implementation for a 3-kW induction motor are completely carried out using a dSpace DS 1104 digital signal processor (DSP) based real-time data acquisition control (DAC) system, and MATLAB/Simulink environment. Digital simulation and experimental results are presented to show the improvement in performance of the proposed algorithm.

Keywords: *Stator flux orientation control (ISFOC), Sensorless vector control, rotor resistance estimation, feedforward decoupling, induction motor drive, Luenberger state-observer (LSO).*

1. Introduction

Due to their high performances in terms of reliability, robustness and efficiency, the adjustable ac-motor drives are increasingly adopted in most industrial applications such as military, aerospace and automotive industries [1]. The aforementioned qualities have been researched and improved by using intelligent and sophisticated control methods based on the field oriented control (FOC) because it adjusts both the amplitude and phase of ac-excitations. The vector control technique has been widely used for high-performance induction motor drives where the knowledge of the rotor speed is necessary. This information is provided by an incremental encoder, which is the most common positioning transducer used today in industrial applications [2, 3].

The use of this sensor implies more electronics, higher cost, lower reliability, difficulty in mounting in some cases such as motor drives in harsh environment and high speed drives, increase in weight, increase in size, and increase in electrical susceptibility.

To overcome these problems, in recent years, the elimination of the transducers has been considered as an attractive prospect. Therefore, numerous approaches have been proposed to estimate the rotor velocity and/or position.

In hottest literature, many researchers have carried out the design of sensorless vector control induction motor drives. These methods, definitely, are based on the following schemes:

Model Reference Adaptive System (MRAS): [4, 7].

Extended Kalman Filters (EKF): [8, 10].

Extended Luenberger observer (ELO): [12, 17].

Newly fuzzy logic and neuronal networks observers [18, 19].

Indeed, some of these methods require specially modified machines and the injection of disturbance signals or the use of a machine model. Otherwise, all other methods for speed estimation using a machine model fed by stator quantities are parameter dependent; therefore, parameter errors can degrade the speed control performance. Thus, some kind of parameter adaptation is required in order to obtain high-performance sensorless vector control drive. At very low speed, indirect stator-flux-oriented control (ISFOC) of induction motor drive is particularly sensitive to an accurate rotor resistance value in the stator flux. To prevail over this problem, online tuning rotor resistance variation of the induction motor is essential in order to maintain the dynamic performance of a sensorless ISFOC drive. Recently, many works dealing with drives without shaft transducers have been developed using different approaches to estimate rotor speed and rotor resistance [11, 20]. Most of these approaches require additional sensors that were not strictly used in standard ISFOC drive; thus, increasing cost and complexity may rule out practical use.

In the very paper, we suggest a contribution to the issue of sensorless indirect stator-flux-oriented control (ISFOC) of IM drive with rotor resistance tuning. The rotor speed and rotor resistance is estimated by the designed-observer by relying on the measured and estimated stator currents and estimated stator fluxes. As a matter of fact, this observer is designed to simultaneously estimate the rotor speed, the rotor resistance, the stator flux and the stator currents. In this respect, the singular perturbation theory is used to get a sequential and simple design of the observer, and the flux observer stability is ensured through the Lyapunov theory. Afterwards, a full description and justification of the proposed algorithm is given and its performances are tested by simulations and experiments. Although related algorithms have previously been presented, the following contributions are believed to be new. First, the dynamic and steady-state performances are analyzed. Excellent behaviour is verified in most cases. Second, the use of the stator field oriented control and a general framework is developed.

This paper is organized as follows: in Section 2, we briefly review the indirect stator-flux-oriented control (ISFOC) of induction motor drives. The procedure design proposed to simultaneous rotor speed and rotor resistance estimation is described in Section 3. Experimental and simulation results are presented in section 4. Finally, in Section 5 we give some comments and conclusions.

2. Stator Flux Orientation Strategy

For ISFOC, the stator flux vector is aligned with d-axis and sets the stator flux to be constant equal to the rated flux, which means $\Phi_{ds} = \Phi_s$ and $\Phi_{qs} = 0$.

2.1 Induction Motor Model

The dynamic model of an induction motor can be represented according to the usual d-axis and q-axis components in synchronous rotating frame as

$$v_{ds} = \frac{R_S(\tau_S+\tau_r)}{\tau_r}\left(1+\frac{\sigma\tau_S\tau_r}{\tau_S+\tau_r}p\right)i_{ds} - \sigma L_s\omega_{sl}i_{qs} - \frac{\Phi_S}{\tau_r} \quad (1)$$

$$v_{ds} = \frac{R_S(\tau_S+\tau_r)}{\tau_r}\left(1+\frac{\sigma\tau_S\tau_r}{\tau_S+\tau_r}p\right)i_{qs} + \sigma L_s\omega_{sl}i_{ds} + \omega_r\Phi_s \quad (2)$$

$$\Phi_s = Ls\frac{1+\sigma\tau_r p}{1+\tau_r p}i_{ds} - \frac{\sigma\tau_r L_S\omega_{sl}}{1+\tau_r p}i_{qs} \quad (3)$$

$$\omega_{sl} = \frac{Ls}{\tau_r}\frac{1+\sigma\tau_r p}{\Phi_S-\sigma L_S i_{ds}}i_{qs} \quad (4)$$

$$T_e = n_p\Phi_s i_{qs} \quad (5)$$

Where $\omega_{sl} = \omega_s - \omega_r$; $\tau_r = \frac{L_r}{R_r}$; $\tau_S = \frac{L_S}{R_S}$; and $\sigma = 1 - \frac{M^2}{L_S L_r}$

It can be perceived that if the stator flux is kept constant, the torque can be controlled by the q-axis current.

The electromagnetic torque equation and the electrical angular speed motor are related by:

$$J\frac{d\omega_r}{dt} + f\omega_r = n_p(T_e - T_l) \quad (6)$$

2.2 Feedforward decoupling controller

It can be seen that the d-axis and q-axis voltage equations are coupled by the terms $-\sigma L_s\omega_{sl}i_{qs} - \frac{\Phi_S}{\tau_r}$ and $\sigma L_s\omega_{sl}i_{ds} + \omega_r\Phi_S$. These terms are considered as disturbances and are cancelled by using a decoupling method that utilizes non-linear feedback of the coupling voltages. If the decoupling method is implemented, the voltage equations become [18].

$$v_d = v_{ds} + e_d = \frac{R_S(\tau_S+\tau_r)}{\tau_r}\left(1+\frac{\sigma\tau_S\tau_r}{\tau_S+\tau_r}p\right)i_{ds} \quad (7)$$

$$v_q = v_{qs} + e_q = \frac{R_S(\tau_S+\tau_r)}{\tau_r}\left(1+\frac{\sigma\tau_S\tau_r}{\tau_S+\tau_r}p\right)i_{qs} \quad (8)$$

Where $e_d = \sigma L_s\omega_{sl}i_{qs} + \frac{\Phi_S}{\tau_r}$ and $e_q = -\sigma L_s\omega_{sl}i_{ds} - \omega_r\Phi_S$; e_d and e_q are, respectively, the d-axis and q-back electromotive force (EMF).

Hence, the dynamics of the d-axis and q-axis currents are now represented by simple linear first-order differential equations. Therefore, it is possible to effectively control the currents with a PI controller.

In Fig. 1, k_{ii} and k_{ip} denote the proportional and integral gains of the PI d, q axis current controller, respectively.

$G_d(p)$, $G_q(p)$ are the no decoupling electrical d, q axis transfer functions of the induction machine. It should be noted that the estimated values, denoted by ^, are introduced to cancel out the coupling terms in the induction motor model.

If we assume that the back EMFs are canceled by the feedforward compensation term, we obtain

$$G_d(p) = G_q(p) = \frac{K_c}{1+\tau_c p} \tag{9}$$

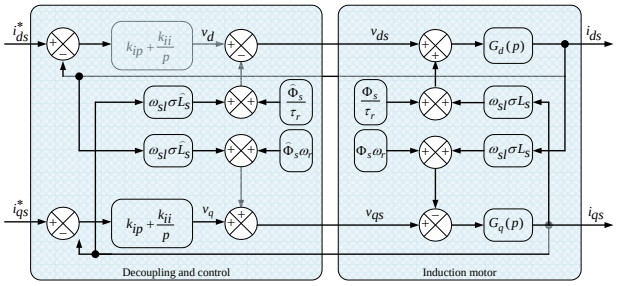

Figure. 1 Block diagram of the conventional PI controller with feed forward decoupling method.

Where $K_c = \frac{\tau_r}{R_s(\tau_s+\tau_r)}$ is a gain and $\tau_c = \frac{\sigma\tau_r\tau_s}{\tau_s+\tau_r}$ is a time constant.

The closed-loop current transfer function is

$$\frac{i_{ds}(p)}{i^*_{ds}(p)} = \frac{i_{qs}(p)}{i^*_{qs}(p)} = \frac{\omega_n^2}{p^2+2\xi\omega_n p+\omega_n^2}\left(1+\frac{k_{ip}}{k_{ii}}p\right) \tag{10}$$

This allows us to write

$$\begin{cases} k_{ii} = \dfrac{\tau_c\omega_n^2}{K_c} \\ k_{ip} = \dfrac{2\xi\tau_c\omega_n - 1}{K_c} \end{cases} \tag{11}$$

Where $\omega_n = \sqrt{\frac{K_c k_{ii}}{\tau_c}}$ and $\xi = \frac{1+K_c+k_{ip}}{2\omega_n\tau_c}$.

ω_n and ξ indicate the natural frequency and damping ratio, respectively. When the dynamics of the d- and q-axes currents are equivalent, the PI gains can be copied to the q-axis controller.

3. Adaptive Luenberger Observer

3.1 Flux observer of induction motor

The state model of the induction motor can be described in a rotating reference frame by:

$$\begin{cases} \dot{x}(t) = \mathbf{A}x(t) + \mathbf{B}v_s(t) \\ y(t) = \mathbf{C}x(t) \end{cases} \tag{12}$$

The adaptive full observer for the estimation of the stator current and the stator flux, using the measured stator currents and voltages, is described by the following set of equations:

$$\begin{cases} \dot{\hat{x}}(t) = \hat{\mathbf{A}}\hat{x}(t) + \mathbf{B}v_s(t) + \mathbf{L}\left[y(t) - \mathbf{C}\hat{x}(t)\right] \\ \hat{y}(t) = \mathbf{C}\hat{x}(t) \end{cases} \tag{13}$$

Where : $\bar{x} = \begin{bmatrix} \bar{i}_{ds} & \bar{i}_{qs} & \bar{\Phi}_{ds} & \bar{\Phi}_{qs} \end{bmatrix}^T$; $x = \begin{bmatrix} i_{ds} & i_{qs} & \Phi_{ds} & \Phi_{qs} \end{bmatrix}^T$;

$\bar{y} = \begin{bmatrix} \bar{i}_{ds} & \bar{i}_{qs} \end{bmatrix}^T$; $y = \begin{bmatrix} i_{ds} & i_{qs} \end{bmatrix}^T$; $v_s(t) = \begin{bmatrix} v_{ds} & v_{qs} \end{bmatrix}^T$

$$\mathbf{A} = \begin{bmatrix} -\gamma\mathbf{I_2} + \omega_r\mathbf{J} & \dfrac{1}{\sigma L_s\tau_r}\mathbf{I_2} - \dfrac{1}{\sigma L_s}\omega_r\mathbf{J} \\ -R_s\mathbf{I_2} & \mathbf{O_2} \end{bmatrix}; \quad \mathbf{B} = \begin{bmatrix} \dfrac{1}{\sigma L_s}\mathbf{I_2} \\ \mathbf{I_2} \end{bmatrix};$$

$\mathbf{C} = \begin{bmatrix} \mathbf{I_2} & \mathbf{O_2} \end{bmatrix}$; $\mathbf{I_2} = \begin{bmatrix} 1 & 0 \\ 0 & 1 \end{bmatrix}$; $\mathbf{J} = \begin{bmatrix} 0 & -1 \\ 1 & 0 \end{bmatrix}$; $\mathbf{O_2} = \begin{bmatrix} 0 & 0 \\ 0 & 0 \end{bmatrix}$ and

$\gamma = \frac{1}{\sigma}\left(\frac{\tau_s+\tau_r}{\tau_s\tau_r}\right)$.

Where ^ alludes to the estimated values, $\hat{x}(t)$ is the observer state vector and $\mathbf{L}$ is the observer gain matrix which is selected so that the system will be stable.

3.2 Luenberger Observer Gain Design

To ensure that the estimation error vanishes over time for any $\tilde{x}(0)$, we should select the observer gain matrix $\mathbf{L}$ so that $(\mathbf{A}-\mathbf{LC})$ is asymptotically stable. Consequently, the observer gain matrix should be chosen so that all eigenvalues of $(\mathbf{A}-\mathbf{LC})$ have real negative parts.

To ensure stability for all ranges of speed, the conventional procedure is to select the observer poles proportional to the motor poles (the proportionality constant is $kp \succ 1$). If the poles of the induction motor are given by λ_{IM} , the observer poles λ_{LO} are selected as:

$$\lambda_{LO} = k_p\lambda_{IM} \tag{14}$$

This can be achieved by defining the observer matrix $\mathbf{L}$ in a special form

$$\mathbf{L} = \begin{bmatrix} l_1\mathbf{I_2} + l_2\mathbf{J} \\ l_3\mathbf{I_2} + l_4\mathbf{J} \end{bmatrix} = \begin{bmatrix} \mathbf{L_1} \\ \mathbf{L_2} \end{bmatrix} \tag{15}$$

To determine the eigenvalues of the matrix $\mathbf{A}$, we use:

$$\det(\lambda_{IM}\mathbf{I_2} - \mathbf{A}) = \begin{vmatrix} \lambda_{IM} + \gamma\mathbf{I_2} - \omega_r\mathbf{J} & -\frac{1}{\sigma L_s \tau_r}\mathbf{I_2} + \frac{1}{\sigma L_s}\mathbf{J} \\ R_s\mathbf{I_2} & \lambda_{IM} \end{vmatrix} = 0 \quad (16)$$

In order to simplify the equation we define

$$a = \gamma\mathbf{I_2} - \omega_r\mathbf{J} \;;\; b = -\frac{1}{\sigma L_s \tau_r}\mathbf{I_2} + \frac{1}{\sigma L_s}\omega_r\mathbf{J} \text{ et } c = R_s\mathbf{I_2}$$

The characteristic equation of the matrix A is then

$$\lambda_{IM}^2 + a\lambda_{IM} - bc = 0 \quad (17)$$

To determine the eigenvalues of the matrix $(\mathbf{A}-\mathbf{LC})$

$$\det(\lambda_{LO}\mathbf{I_2} - (\mathbf{A}-\mathbf{LC})) = \begin{vmatrix} \lambda_{IM} + \gamma\mathbf{I_2} - \omega_r\mathbf{J} + \mathbf{L_1} & -\frac{1}{\sigma L_s \tau_r}\mathbf{I_2} + \frac{1}{\sigma L_s}\mathbf{J} \\ R_s\mathbf{I_2} + \mathbf{L_2} & \lambda_{LO} \end{vmatrix} = 0 \quad (18)$$

Hence, the characteristic equation is

$$\lambda_{LO}^2 + \lambda_{LO}(\mathbf{L_1} + a) - b(\mathbf{L_2} + c) = 0 \quad (19)$$

The substitution of Eq. (16) in (21) yields

$$k_p^2\lambda_{IM}^2 + k_p\lambda_{IM}(\mathbf{L_1} + a) - b(\mathbf{L_2} + c) = 0 \quad (20)$$

The identification of Eq. (22) and k_p^2* (19) gives the following results:

$$\begin{cases} l_1 = (k_p - 1)\gamma \\ l_2 = (k_p - 1)\hat{\omega}_r \\ l_3 = (k_p^2 - 1)R_s \\ l_4 = 0 \end{cases} \quad (21)$$

3.3 Adaptive Flux Observer for Speed Estimation

When the motor speed is not measured, it is treated as an unknown parameter in the observer (13). By adding an adaptive scheme for estimating the rotor speed to the observer, both states and unknown parameters can be estimated simultaneously. The adaptive scheme is derived using Lyapunov theory. From (12) and (13), the estimation error of the stator and rotor flux is given by the following equation:

$$\dot{e} = (\mathbf{A} + \mathbf{LC})e + (\quad)x \quad (22)$$

Where $e = x - \hat{x}$; $\Delta\mathbf{A} = \mathbf{A} - \hat{\mathbf{A}} = \begin{bmatrix} \Delta\omega_r\mathbf{J} & -\frac{1}{\sigma L_s}\Delta\omega_r\mathbf{J} \\ 0 & 0 \end{bmatrix}$ and

$\Delta\omega_r = \omega_r - \hat{\omega}_r$

We define a Lyapunov function candidate V

$$V = e_n^T e_n + \frac{(\hat{\omega}_r - \omega_r)^2}{\lambda} \quad (23)$$

Where λ is a positive constant and

$e_n = \begin{bmatrix} i_S - \hat{i}_S & \Phi_S - \hat{\Phi}_S \end{bmatrix} = \begin{bmatrix} e_{i_S} & e_{\Phi_S} \end{bmatrix} = \mathbf{\Gamma}e$

With $\mathbf{\Gamma}$ a nonsingular matrix

For the derivation of the adaptive mechanism, the unknown parameter $\hat{\omega}_r$ is considered constant. The time derivative of V becomes

$$\dot{V} = e_n^T\left\{\left[\mathbf{\Gamma}\left(\mathbf{A}+\mathbf{LC}\right)\mathbf{\Gamma}^{-1}\right]^T + \left[\mathbf{\Gamma}\left(\mathbf{A}+\mathbf{LC}\right)\mathbf{\Gamma}^{-1}\right]\right\}e_n + 2\frac{\Delta\omega_r}{\sigma L_S}(\hat{\Phi}_{\beta s}e_{i_{\alpha s}} - \hat{\Phi}_{\alpha s}e_{i_{\beta s}}) - \frac{2}{\lambda}\Delta\omega_r\frac{d\hat{\omega}_r}{dt} \quad (24)$$

The adaptive scheme for speed estimation is given by:

$$\hat{\omega}_r = K_{P\omega_r}\left(\hat{\Phi}_{\beta s}e_{\alpha s} - \hat{\Phi}_{\alpha s}e_{i_{\beta s}}\right) + K_{I\omega_r}\int_0^t\left(\hat{\Phi}_{\beta s}e_{i_{\alpha s}} - \hat{\Phi}_{\alpha s}e_{i_{\beta s}}\right)dt \quad (25)$$

The adaptive flux observer is stable according to the Lyapunov direct method if the observer gain is chosen such that the first term of (24) is negative semidefinite. This condition is fulfilled if the eigenvalues of $\mathbf{\Gamma}(\mathbf{A}+\mathbf{LC})\mathbf{\Gamma}^{-1}$ have negative real parts. Since the eigenvalues of $\mathbf{\Gamma}(\mathbf{A}+\mathbf{LC})\mathbf{\Gamma}^{-1}$ equal the eigenvalues of $(\mathbf{A}+\mathbf{LC})$ ($\mathbf{\Gamma}$ is nonsingular), the observer should have stable poles.

3.4 Adaptive Flux Observer for Speed and Rotor Resistance Estimation

Due to temperature changes during operation, the IM stator resistance and rotor resistance will vary. The proposed adaptive observer can be extended to include rotor resistance estimation. When both rotor resistance and speed are treated as unknown parameters of the observer, the estimation error of the stator and rotor flux is calculated from (12) and (13) and is provided by the following equation.

$$\dot{e} = (\mathbf{A} + \mathbf{LC})e + \Delta\mathbf{A}'x + \quad 'x \quad (26)$$

Where

$\Delta\mathbf{A}' = \begin{bmatrix} -\frac{\Delta R_r}{\sigma L_r}\mathbf{I_2} & \frac{\Delta R_r}{\sigma L_S L_r}\mathbf{I_2} \\ \mathbf{0_2} & \mathbf{0_2} \end{bmatrix}$ and $\Delta R_r = R_r - \hat{R}_r$

A Lyapunov function candidate V' is defined as follows:

$$V' = e_n^T e_n + \frac{(\hat{\omega}_r - \omega_r)^2}{\lambda} + \frac{(\hat{R}_r - R_r)^2}{\lambda'} = V + \frac{(\hat{R}_r - R_r)^2}{\lambda'} \quad (27)$$

and its time derivative is

$$\dot{V}' = \dot{V} + \hat{x}^T \mathbf{\Delta A}'^T \mathbf{\Gamma}^T e_n + e_n^T \mathbf{\Gamma \Delta A}' \hat{x}$$
$$-2\frac{\Delta R_r}{\sigma L_r L_s} e_{i\alpha s} (\hat{\Phi}_{\alpha s} - Ls\hat{i}_{\alpha s}) \quad (28)$$
$$-2\frac{\Delta R_r}{\sigma L_r L_s} e_{i\beta s} (\hat{\Phi}_{\beta s} - Ls\hat{i}_{\beta s}) + 2\frac{\Delta R_r}{\lambda'}\frac{d\hat{R}_r}{dt}$$

The adaptive scheme for rotor resistance estimation is found by equating the second and third term in (28)

$$\hat{R}_r = K_{PR_r}\left[e_{i\alpha s}(\hat{\Phi}_{\alpha s} - Ls\hat{i}_{\alpha s}) + e_{i\beta s}(\hat{\Phi}_{\beta s} - Ls\hat{i}_{\beta s})\right]$$
$$+K_{IR_r}\int_0^t \left[e_{i\alpha s}(\hat{\Phi}_{\alpha s} - Ls\hat{i}_{\alpha s}) + e_{i\beta s}(\hat{\Phi}_{\beta s} - Ls\hat{i}_{\beta s})\right]dt \quad (29)$$

The structure of the proposed adaptive observer for speed and rotor resistance estimation is shown in Fig. 2.

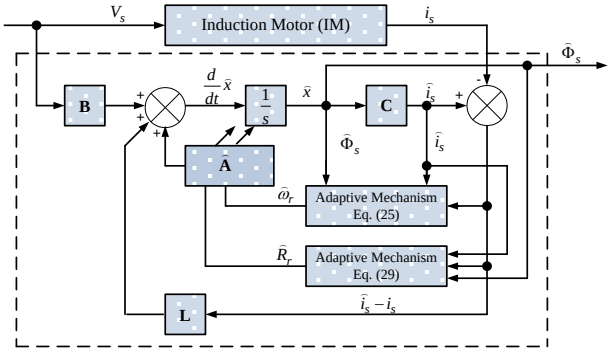

Figure. 2 Block diagram of combined speed and rotor resistance estimation.

4. Simulation and experimental results

In this section, some simulation and experimental results are presented to evaluate the effectiveness of the proposed control scheme for an induction motor. Figure 3 shows the block diagram of the proposed sensorless ISFOC with rotor resistance tuning of induction motor drive system. The bloc diagram consists of an induction motor, a PWM voltage source inverter, a field orientation algorithm, a coordinate translator, and a speed controller.

To implement the proposed sensorless ISFOC with rotor resistance tuning of induction motor drive, an experimental testing ground was carried out. It is essentially composed of:

- An induction motor a 3-kW whose parameters are listed in appendix.
- A static power electronics convertor from semikron composed of a diode rectifier and a three-leg voltage source IGBT inverter.
- Current sensors of Hall.
- A dSpace DS 1104 ACE Kit with control desk software plugged in a Pentuim 4 personal computer.

For the implementation of the proposed sensorless ISFOC ISFOC with rotor resistance tuning of induction motor drive, an experimental has been carried out (Fig. 4). The sensorless ISFOC algorithm which is programmed with Matlab-Simulink and downloaded in the dSpace 1104 control board offers a four-channel 16-bit (multiplexed) ADC and four 12-bit ADC units. A sampling period of 50µs is selected and the insulated gate bipolar transistors (IGBTs) are working at a switching frequency of 10 kHz with a dead time of 20µs. The load is generated through a magnetic powder brake coupled to the induction motor. The output control signals of the Slave I/O PWM are of TTL level 5V, whereas IGBTs of the static inverter must receive signals of 15V. Additionally, an adaptation interface board using the integrated circuit IR2130 from International rectifier is realized.

In order to check the validity of the implementation of ISFOC with rotor resistance tuning of induction motor drive using dSpace DS 1104 control board, some simulation and experimental works have been performed. The flux is kept constant at its rated value 1.21Wb. The first aim of the present simulation and experimental results is to test the performance of the sensorless ISFOC with rotor resistance tuning of induction motor drive system for a reference speed ±1000 rpm with load torque equal 20 N.m applied and removed at t = 6.5 and 16.5 s, respectively.

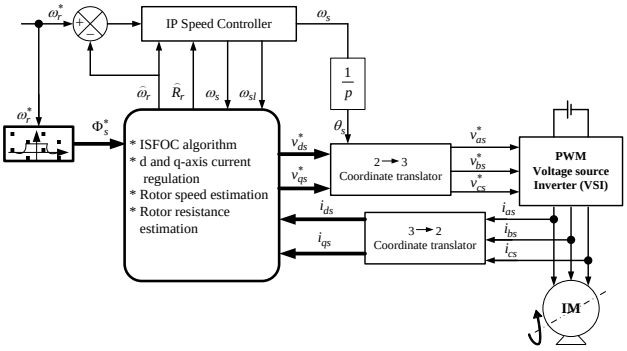

Figure.3 Block diagram of sensorless (ISFOC) with rotor resistance tuning of induction motor drive system.

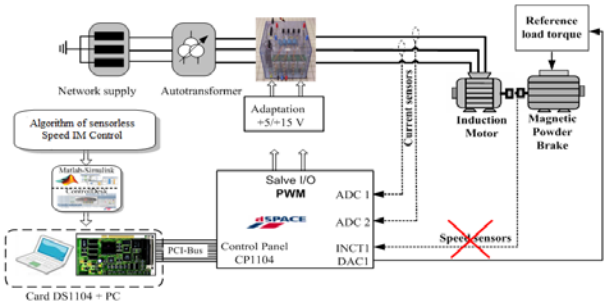

Figure.4 Scheme used for experimental setup.

The IP speed controller is designed to stabilize the speed control loop. Moreover, the gains of the IP controller are determined by using a design method to obtain a damping ratio of 1.

As a first test, Fig. 5 shows the simulation and experimental results for sensorless (ISFOC) with rotor resistance tuning of induction motor drive. Accordingly, when the speed command changes from zero to (1000 rpm) in forward rotation, it changes to reverse direction of the same speed.

In Figs. 5(a) and (b), the simulation and experimental results of the reference, estimated and actual rotor speed, and in Fig. 5(c) and (d), simulation and estimated results of d-axis and q-axis stator flux, are presented. The estimated d, q components of stator flux are obtained from the stator voltage model of induction motor in d, q reference frame. Besides, simulation and measured results of d-q axis currents are given in Figs. 5(e) and (f). Fig. 5(g) and (h) shows, respectively, simulation results and experimental of estimated rotor resistance.

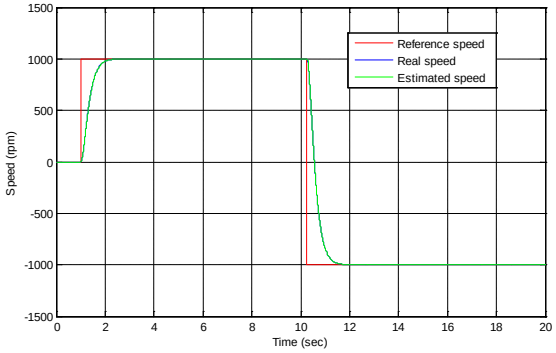

(a) simulated

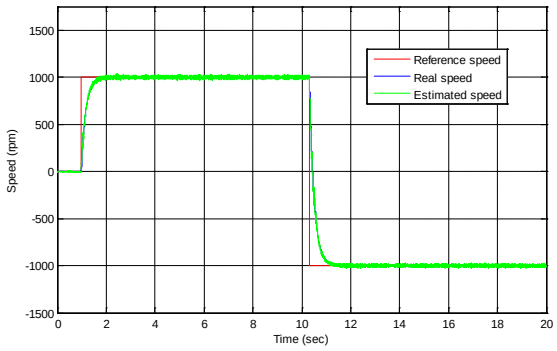

(b) experimental

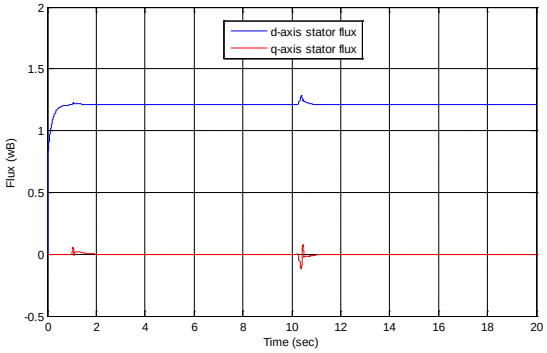

(c) simulated

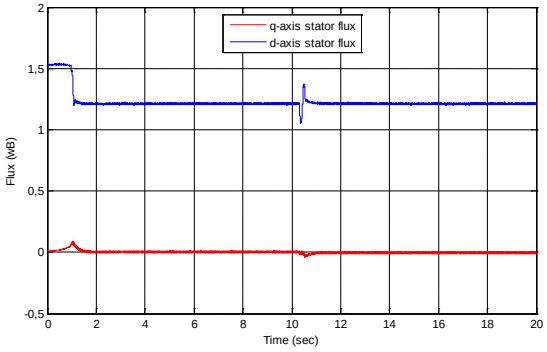

(d) experimental

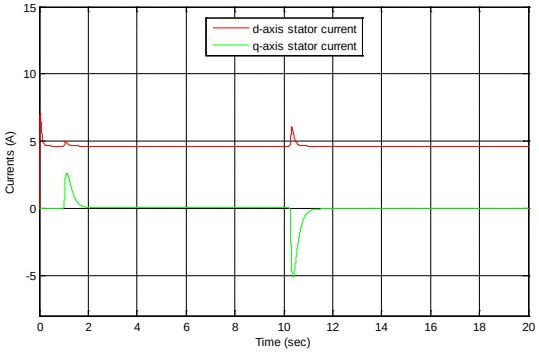

(e) simulated

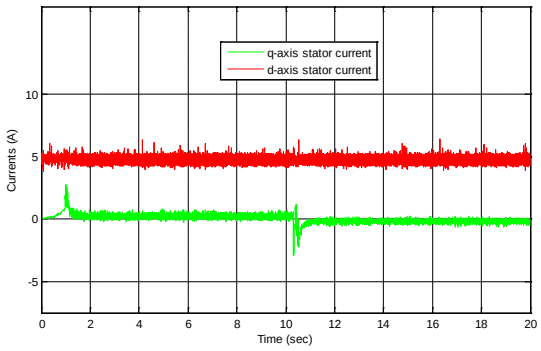

(f) experimental

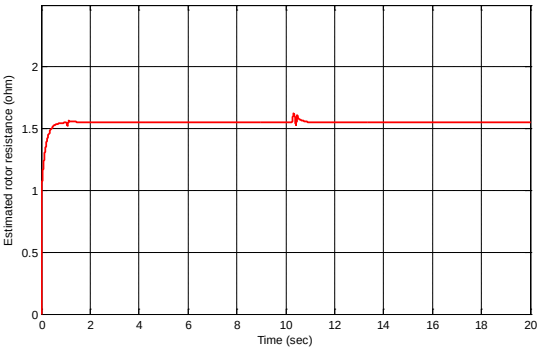

(g) simulated

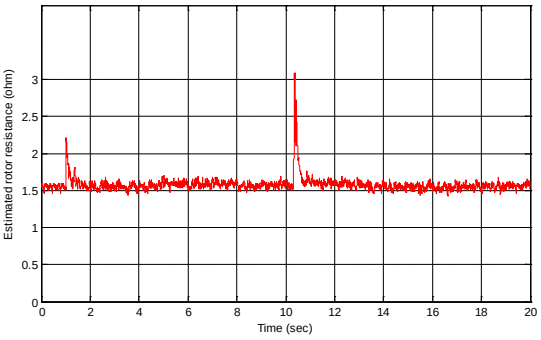

(h) experimental

Figure.5 Experimental and simulation results of sensorless (ISFOC) (no load) with rotor resistance tuning for reversing speed reference from 1000rpm to -1000rpm.

As a second test, some simulation and experimental results for sensorless (ISFOC) with rotor resistance tuning of induction motor drive are presented in Fig. 6 for 1000 rpm speed reference command and a load torque of 20 N.m is applied and removed at t=6.5 and 16.5s, respectively. In Figs. 6(a) and (b), the simulation and experimental results of the reference, real and estimated rotor speed, and in Figs. 6(c) and (d), the simulation and estimated results of d-axis and q-axis stator flux, are presented a load torque variation. In Figs. 6(e) and (f), the simulation and experimental results of d-q axis currents are presented. Furthermore, the simulation results and measured stator phase currents are given in Figs. 6(g) and (h). Figs. 6(i) and (j) show, respectively, the simulation results and measurement of load torque and q-axis stator current. Fig. 6(k) and (l) shows, respectively, the simulation and experimental results of estimated rotor resistance.

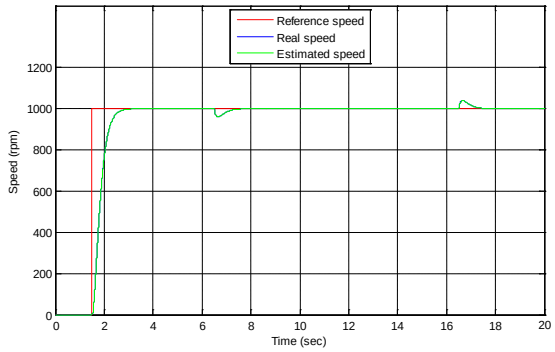

(a) simulated

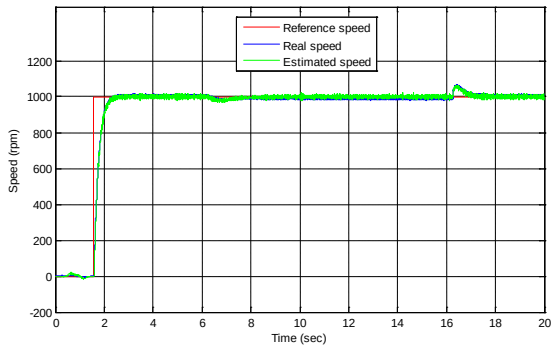

(b) experimental

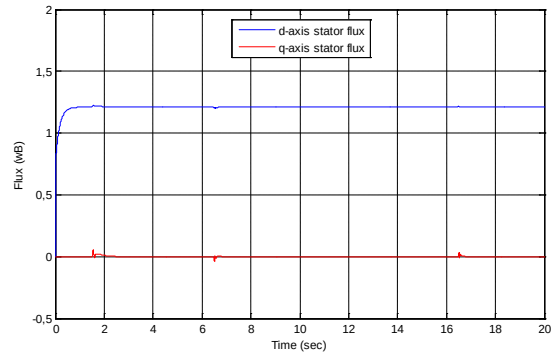

(c) simulated

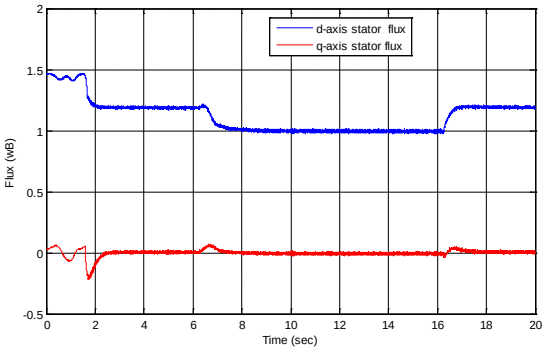

(d) Experimental

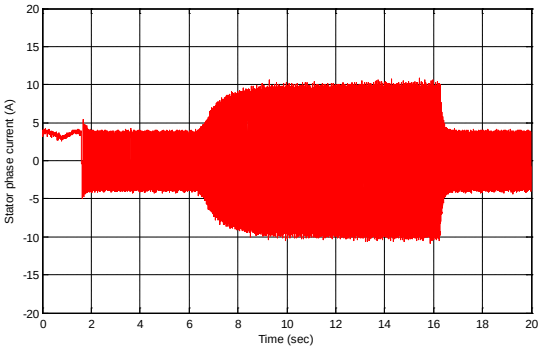

(h) Experimental

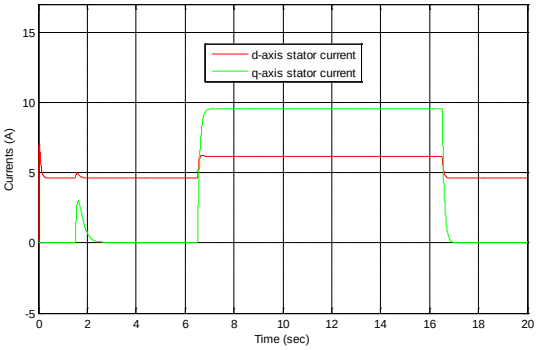

(e) simulated

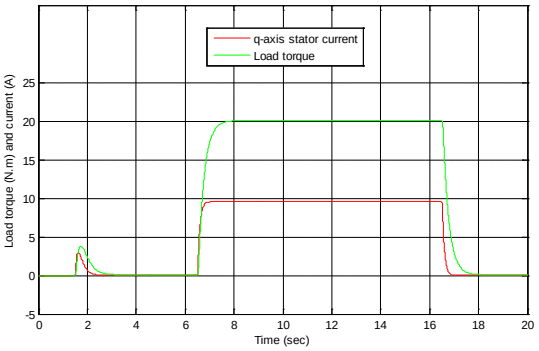

(i) simulated

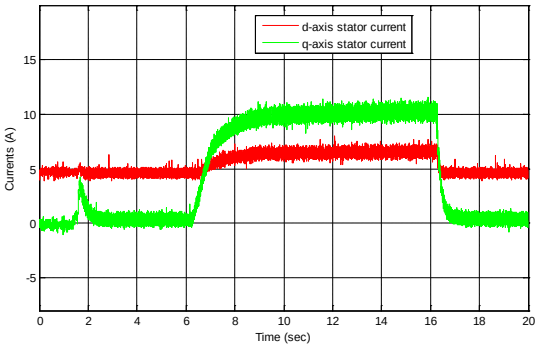

(f) Experimental

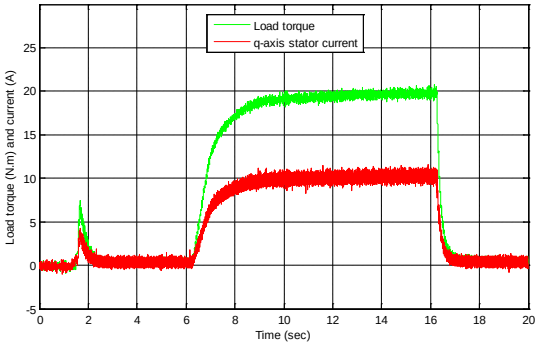

(j) Experimental

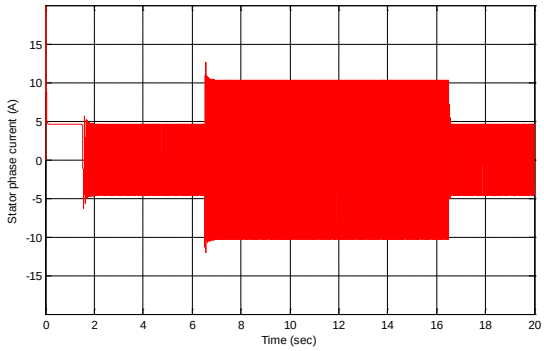

(g) simulated

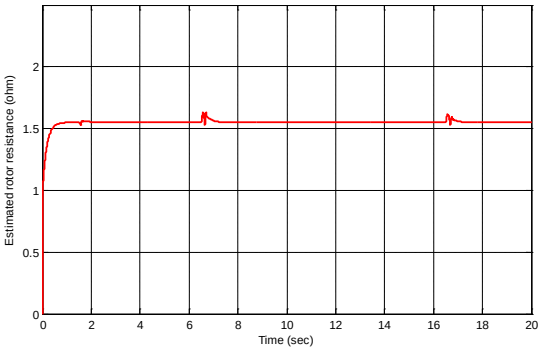

(k) simulated

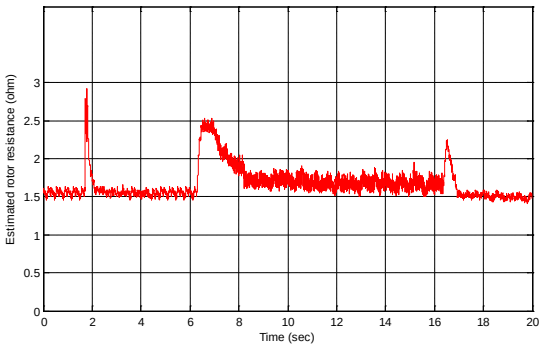

(l) Experimental

Figure.6 Experimental and simulation results of sensorless (ISFOC) (with load torque of 20 N.m applied at 6.5 s) with rotor resistance tuning the speed command is 1000 rpm

In steady state operation, it should be noted that in Fig. 6(c) and (d) the d-axis stator flux builds up to the rated value (1.21 wB) by d-axis stator current, while q-axis stator flux and current components remain zero. This shows that a decoupling between stator flux and the torque is achieved. It should also be noted that we have considered the stator resistance to be constant. However, like stator resistance, rotor resistance also depends on temperature. It is clear that an improvement of high performance sensorless speed control requires tracking changes in stator resistance.

5. Conclusions

In this paper, one has validated the online simultaneous estimation of speed and rotor resistance in sensorless indirect stator flux orientation control of induction motor drive system based on Luenberger observer. In other words, the complexity of the algorithm is reduced by using analytical relations to obtain directly the Luenberger observer (LO) gain matrix as a function of the electrical velocity and the proportional constant. The validity of the proposed sensorless ISFOC of induction motor drive with rotor resistance tuning was also proven by simulation and experiments for a wide range of speed. More importantly, all experimental results confirm the good dynamic performances of the developed drive systems and show the validity of the suggested method. It is concluded from the results presented in this paper that the proposed scheme performs well for both high and low speed.

Appendix

List of motor specification and parameters: 220/380V, 3kW, 4 poles, 1430 rpm

$R_s = 2.3\Omega$; $R_r = 1.55\Omega$; $L_s = L_r = 0.261H$; $M = 0.245H$; $f = 0.002 Nm.s.rd^{-1}$; $J = 0.03 kg.m^2$.

References

[1] J. Jung, K. Nam, "A dynamic decoupling control scheme for high speed operation of induction motor", IEEE Transaction on Industry Applications, Vol. 30, 1994, pp. 1219– 1224.

[2] F. J. Lin, R. J. Wai, C. H. Lin, and D. C. Liu, "Decoupling stator-flux oriented induction motor drive with fuzzy neural network uncertainly observer", IEEE Transaction on Industrial Electronics, Vol. 47, No. 2, 2000, pp. 356– 367.

[3] S. Suwankawin and S. Sangwongwanich, "A speed sensorless IM drive with decoupling control and stability analysis of speed estimation", IEEE Transaction on Industrial Electronics, Vol. 49, No. 2, 2002, pp. 444– 455.

[4] Y. Agrebi, M. Triki, Y. Koubaa, M. Boussak, "Rotor speed estimation for indirect stator flux oriented induction motor drive based on MRAS Scheme", Journal of Electrical Systems, 2007, Vol. 3, pp. 131– 143.

[5] R. Blasco-Giménez, G. Asher, M. Summer, K. Bradley, "Dynamic performance limitations for MRAS based sensorless induction motor drives. Part 1: Stability analysis for the closed loop drive", IEEE Proceeding of Electric Power Applications, Vol. 143, 1996, pp. 113– 122.

[6] Y. Koubaa, M. Boussak, "Rotor resistance tuning for indirect stator flux oriented induction motor drive based on MRAS scheme", Revue European Transactions on Electrical Power, Vol. 15, No. 6, 2005, pp. 557– 570.

[7] L. Zhen and L. Xu, "Sensorless field orientation control of induction machines based on mutual MRAS scheme", IEEE Transaction on Industry Applications, Vol. 45, No. 5, 1998, pp. 824– 831.

[8] Y. R. Kim, S. K. Sul, and M. H. Park, "Speed sensorless vector control of induction motor using an extended Kalman filter", IEEE Transaction on Industry Applications, Vol. 30, No. 5, 1994, pp. 1225– 1233.

[9] K. L. Shi, Y. K. Wong, and S. L. Ho, "Speed estimation of an induction motor drive using an optimized extended Kalman filter", IEEE Transaction on Industrial Electronics, Vol. 49, No. 1, 2002, pp. 124– 133.

[10] L.C. Zai, C.L. Demarco, T.A. Lipo, "An extended Kalman filter approach to rotor time-constant measurement in PWM induction motor drives", IEEE Transaction on Industrial Electronics, Vol. 28, No. 1, 1992, pp. 96– 104.

[11] K. Akatsu, A. Kawamura, "Online rotor resistance estimation using the transient state under the speed sensorless control of induction motor", IEEE Transaction on Power Electronics, Vol. 15, No. 3, 2000, pp. 553– 560.

[12] L. Jingchuan, L. Xu, Z. Zhang, "An adaptive sliding-mode observer for induction motor sensorless speed control", IEEE Transaction on Industrial Electronics, Vol. 46, No. 1, 1999, pp. 100– 110.

[13] H. Kubota K. Matsuse, "Speed sensorless field-oriented control of induction motor with rotor resistance adaptation", IEEE Transaction on Industrial Electronics, Vol. 30, No. 5, 1994, pp. 1219– 1224.

[14] H. Kubota, K. Matsuse, T. Nakano, "Dsp-based speed adaptive flux observer of induction motor", IEEE

Transaction on Industrial Electronics, Vol. 29, 1993, pp. 344– 348.
[15] D.J. Atkinson, J.W. Finch, P.P. Acamley, "Estimation of rotor resistance in induction motor", IEE Proceedings Electric Power Applications, Vol. 143, No. 1, 1996, pp. 87– 94.
[16] T. Du, P. Vas, F. Stronach, "Design and application of extended observers for joint state and parameter estimation in high-performance AC drivers", IEE Proceedings Electric Power Applications, Vol. 142, No. 2, 1995, pp. 71– 78.
[17] T.O Kowalska, "Application of extended Luenberger observer for flux and rotor time-constant estimation in induction motor drives", IEE Proceedings on Control Theory and Applications, Vol. 136, No. 6, 1989, pp. 324– 330.
[18] H. Rehman, R. Dhaouadi, A fuzzy learning-Sliding mode controller for direct field-oriented induction machines, Neurocomputing. 71 (2008) 2693– 2701.
[19] B. Karanayil, M. F. Rahman, and C. Grantham, "Online stator and rotor resistance estimation scheme using artificial neural networks for vector controlled speed sensorless induction motor drive", IEEE Transaction on Industrial Electronics, Vol. 54, No. 1, 2007, pp. 167– 176.
[20] M. Boussak, K. Jarray, "A High-Performance Sensorless Indirect Stator Flux Orientation of Induction Motor Drive", IEEE Transaction on Industrial Electronics, Vol. 53, No. 1, 2006, pp. 41– 49.

Mabrouk Jouili was born in Ben Guerdane, Tunisia, on August 14, 1980. He received the Engineer degree and the M.S. degree in electrical engineering from the Ecole Nationale d'Ingénieurs de Sfax (ENIS), Tunisia, in 2005 and 2007, respectively. In September 2008, he is inscribed in doctor's degree in the field of electrical engineering at the Ecole Nationale d'Ingénieurs de Sfax (ENIS), Sfax, Tunisia. Since 2007, he is an Assistant teacher at the Institut Supérieur d'Informatique de Médenine, Tunisia. His current research interests include electric machines, fault detection and localization, observation and sonsorless control.

Kamel Jarray was born in Ben Guerdane, Tunisia, on June 18, 1967. He received the B.S. and DEA degrees from the Ecole Supérieure des Sciences et Techniques de Tunis (ESSTT), Tunis, Tunisia, in 1993 and 1995, respectively, and the Ph.D. degree from Aix-Marseille III University, Marseille, France, in 2000, all in electrical engineering. From 2000 to 2001, he was a Researcher at the Ecole Supérieure d'Ingénieurs de Marseille (ESIM). From 2001 to 2003, he was an Assistant Professor at the Ecole Supérieure des Sciences et Techniques de Tunis (ESSTT), Tunisia. Since September 2003, he has been an Assistant Professor at the Ecole Nationale d'Ingénieurs de Gabès (ENIG), Gabès, Tunisia. His research is in the areas of electrical machines, sensorless vector control ac motor drives, and advanced digital motion control.

Yassine Koubaa is the Head of Automatic Control Research Laboratory (Sfax-Tunisia) and the Editor in Chief of International Journal on Sciences and Techniques of Automatic control & computer engineering (IJ-STA). He received the B.S.and DEA (master) degrees in 84 and 86, respectively, the Doctorat theses in 1996, the "Habilitation Universitaire" (HDR) from the National Engineering school of Sfax (ENIS) all in Electrical Engineering. From 1989 to 1996, he was an Assistant Professor in the Electrical Engineering Department of ENIS. In September 1997, he became an Associate Professor. Since September 2005, he is a full professor at the same university. His main research interests cover several aspects related to electrical machines, including systems identification, advanced motion control and diagnostics. He has authored more than 70 papers in international conferences and technical Journals in the area as well as many patents. He serves as a member of the Scientific and the Technical Program Committees of several international conferences and technical Journals in the motor drives fields.

Mohamed Boussak currently serves as a Member of the Technical program committees of several international conferences and scientific Journals in the areas of power electronics and motor drives fields. He received the B.S. and DEA degrees from the Ecole Normale Supérieure de l'Enseignement Technique de Tunis (ENSET), Tunisia, in 1983 and 1985 respectively, the Ph.D.degree from Pierre et Marie Curie University (Paris 6), Paris, France, in 1989, the "Habilitation à Diriger des Recherches" (HDR) from Aix-Marseille III University, Marseille, France in 2004, all in Electrical Engineering. From September 1989 to September 1990, he was a Researcher with the Ecole Supérieure d'Ingénieurs de Marseille ESIM. From October 1990 to September 1991, he was a Research Teacher in Electrical Engineering with the Claude Bernard University, Lyon, France. From October 1991 to June 2004, he was an Associate Professor with the Ecole Supérieure d'Ingénieurs de Marseille (ESIM), France. From July 2004 to December 2008, he was an Associate Professor of Electrical Machines with the Ecole Centrale Marseille (ECM), France, where, since January 2009, he has been a Senior Professor. His research areas, in the Laboratoire des Sciences de l'Information et des Systèmes (LSIS), UMR CNRS 6168, Marseille, France, are electrical machines, power conversion systems, sensorless vector control ac motor drives, advanced digital motion control and diagnostic for industrial electric system. He has published more than 100 papers in scientific Journals and conference proceedings in these research fields. Dr. Boussak is Senior Member of IEEE Industry Application, IEEE Industrial Electronics and IEEE Power Electronics Societies.